Concurrent induction of apoptosis and necroptosis in apigenin-treated malignant mesothelioma cells: Reversal of Warburg effect through Akt inhibition and p53 upregulation

YOON-JIN LEE[1], KWAN-SIK PARK[1], SU-HAK HEO[2], MOON-KYUN CHO[3] and SANG-HAN LEE[1]

[1]Department of Biochemistry, College of Medicine, Soonchunhyang University, Cheonan 31151; [2]Department of Medicinal Bioscience, College of Biomedical and Health Science, Konguk University Glocal Campus, Chungju 27478; [3]Department of Dermatology, Soonchunhyang University Seoul Hospital, Seoul 04401, Republic of Korea

Abstract. A high dependence on aerobic glycolysis, known as the Warburg effect, is one of the metabolic features exhibited by tumor cells. Therefore, targeting glycolysis is becoming a very promising strategy for the development of anticancer drugs. In the present study, it was investigated whether pre-adaptation of malignant mesothelioma (MM) cells to an acidic environment was associated with a metabolic shift to the Warburg phenotype in energy production, and whether apigenin targets acidosis-driven metabolic reprogramming. Cell viability, glycolytic activity, Annexin V-PE binding activity, reactive oxygen species (ROS) levels, mitochondrial membrane potential, ATP content, western blot analysis and spheroid viability were assessed in the present study. MM cells pre-adapted to lactic acid were resistant to the anticancer drug gemcitabine, increased Akt activation, downregulated p53 expression, and upregulated rate-limiting enzymes in glucose metabolism compared with their parental cells. Apigenin treatment increased cytotoxicity, Akt inactivation and p53 upregulation. Apigenin also reduced glucose uptake along with downregulation of key regulatory enzymes in glycolysis, increased ROS levels with loss of mitochondrial membrane potential, and downregulated the levels of complexes I, III and IV in the mitochondrial electron transport chain with intracellular ATP depletion, resulting in upregulation of molecules mediating apoptosis and necroptosis. Apigenin-induced alterations of cellular responses were similar to those of Akt inactivation by Ly294002. Overall, the present results provide mechanistic evidence supporting the anti-glycolytic and cytotoxic role of apigenin via inhibition of the PI3K/Akt signaling pathway and p53 upregulation.

Introduction

Living organisms require a continuous influx of energy to perform the various physiological activities necessary for cell growth and survival. Adenosine triphosphate (ATP), the energy currency of cells, is produced by glycolysis in the cytoplasm and oxidative phosphorylation in the mitochondria. Both processes occur essentially in most cells. However, oxidative phosphorylation predominates, and glycolysis is increased when there is insufficient oxygen supply, such as in muscle cells during exercise. However, tumor cells rely more on glycolysis than oxidative phosphorylation for ATP production even under adequate oxygenation, which is called the Warburg effect (1). Depending on the cancer type, a variety of intracellular and extracellular changes, including mitochondrial alterations, upregulation of key glycolytic enzymes, intracellular pH control and hypoxia-induced conversion to anaerobic metabolism, have been shown to mediate the Warburg effect (2,3). Metabolic shift to aerobic glycolysis provides intermediates for various biosynthetic pathways and adapts cancer cells to hypoxic conditions in solid tumors (4). Enhanced glycolysis in tumor cells increases lactic acid accumulation and acidity in the extracellular compartment in tumor, which significantly contributes to resistance to chemotherapy, proliferation and metastasis (5).

The phosphatidylinositide 3-kinase (PI3K)/protein kinase B (Akt) pathway regulates various cellular processes including cell survival, proliferation, metabolism, motility and apoptosis (6). It is initiated by autophosphorylation of the tyrosine residue in the receptor protein tyrosine kinases, and is found to be frequently activated in human cancers. In particular, activation of the PI3K/Akt/mammalian target of rapamycin (mTOR) signaling pathway plays an essential role in triggering the Warburg effect in tumor cells by increasing the activity and expression of glucose transporters (GLUTs) and glycolytic enzymes (7,8) without affecting mitochondrial oxidative phosphorylation (9). The PI3K/Akt/mTOR pathway is frequently activated in malignant mesothelioma (MM),

Correspondence to: Dr Sang-Han Lee, Department of Biochemistry, College of Medicine, Soonchunhyang University, 31 Soonchunhyang 6-gil, Dongnam, Cheonan 31151, Republic of Korea
E-mail: m1037624@sch.ac.kr

presumably due to reactive oxygen species (ROS)-mediated inactivation of phosphatase and tensin homolog (PTEN) (10). However, little is known about an association of the Warburg effect with the PI3K/Akt/mTOR pathway in MM. An intricate interplay exists between the Akt and p53 pathways. Under appropriate survival signals, Akt negatively modulates the tumor suppressor p53 levels by enhancing the murine double minute 2 (MDM2)-mediated degradation of p53 (11). p53 antagonizes PI3K/Akt signaling by inducing the expression of PTEN, enabling cells to undergo rapid apoptosis (12). Therefore, mutations that activate the PI3K/Akt signaling pathway and inactivate the p53 gene are common mechanisms to increase cancer cell survival and form more malignant clones, and targeting Akt has become a key strategy in cancer therapy and prevention (13).

Apigenin (4',5,7-trihydroxyflavone) not only induces apoptosis, autophagy, cell cycle arrest, but also inhibits angiogenesis and metastasis in different types of cancer cells (14,15). Several signaling pathways including PI3K/Akt, nuclear factor kappa B (NF-kB), and mitogen-activated protein kinase/extracellular signal-regulated kinase (MAPK/ERK) are known to modulate apigenin activity (15). Among them, the importance of the PI3K/Akt pathway as a major molecular target for the various anticancer activities of apigenin has been demonstrated in *in vitro* and *in vivo* studies (14,16). Little is known about the effect of apigenin in MM, but a previous study revealed that it induces apoptosis by inhibiting the c-Jun N-terminal kinase (JNK) pathway (17). Recently, it was demonstrated by the authors that apigenin induces apoptosis and necroptosis of MM cells with intracellular ROS accumulation, mitochondrial dysfunction and ATP depletion at a concentration of 30 μM that does not affect normal mesothelial MeT-5A cells (18).

A variety of evidence indicates that inhibition of glycolysis in cancer cells results in ATP depletion and cell death, which is particularly effective in cells with high glycolytic activity and resistance to anticancer drugs (19,20). Severe ATP depletion is more likely to cause cell death through necrosis rather than apoptosis (19,21). A distinct shift in energy metabolism towards the Warburg profile was also observed in MM tissues, as characterized by increased expression of numerous genes involved in glycolysis and oxidative metabolism and the accumulation of 2-deoxy-2-[fluorine-18] fluoro-D-glucose in tumor lesions in positron emission tomography analysis (10,22). Furthermore, MM cell lines, including MSTO-211H and H2452 cells, have been shown to depend on glucose metabolism for rapid growth (23). Together with the authors' previous findings linking apigenin-induced cell death with mitochondrial dysfunction and ATP depletion, the results of the aforementioned studies led us to the hypothesis that the effects of apigenin on energy metabolism are mediated by targeting glycolysis through inhibition of the PI3K/Akt pathway.

In the present study, it was aimed to extend the previous investigation into the anticancer role of apigenin and to evaluate its effects on energy metabolism and cell death using two human MM cell lines pre-adapted to lactate. The cell lines were established by continuously exposing MSTO-211H and H2452 cells to 3.8 μM lactic acid through 4 serial passages for 15 days. The current data provide mechanistic evidence suggesting a close link between the PI3K/Akt pathway, p53

and glycolysis in the induction of apoptosis and necroptosis. The current study deepens our understanding of the novel role of apigenin in MM cells.

Materials and methods

Cell culture and assays. Human MM cell lines MSTO-211H and H2452 were purchased from the American Type Culture Collection. Acidic pre-adapted cells designated as MSTO-211HAcT (cat. no. CRL-2081) and H2452AcT (cat. no. CRL-5946) were established by continuously exposing MSTO-211H and H2452 cells, respectively, to 3.8 μM lactic acid through 4 passages for 15 days. Cells were cultured in in RPMI-1640 medium (Welgene, Inc.) containing 3.8 μM lactic acid and 5% fetal bovine serum (Welgene, Inc.), and then treated with increasing concentrations (10, 20, 40, 80 and 160 μM) of gemcitabine for cell viability assay. Cells were treated with 20 μM Ly294002 (Merck KGaA) and 30 μM apigenin (MilliporeSigma) alone or in combination for 48 h. For combination treatment, pretreatment with Ly294002 for 2 h followed by treatment with apigenin without removing Ly294002. As a negative control, cells were treated with 0.1% dimethyl sulfoxide. Cell viability was measured by MTT assay as previously described (18). The activities of hexokinase (HK) and pyruvate dehydrogenase (PDH) were determined using an HK Colorimetric Assay Kit (cat. no. K789-100) and PDH Activity Colorimetric Assay Kit (cat. no. K679-100), respectively, according to the protocols provided by the manufacturer (BioVision, Inc.). Glucose consumption was determined by assessing the glucose content in the culture media according to the instruction provided in the Glucose Colorimetric Assay Kit (cat. no. K606-100; Biovision, Inc.). Nuclear morphology of apoptotic cells, such as nuclear fragmentation and chromosome condensation, was observed in cells stained with 2',7'-dichlorodihydrofluorescein iodide (DAPI, 2 μg/ml) for 10 min in the dark as previously described by Lee *et al* (24). Intracellular ATP content was determined by luminescence measurement using the CellTiter-Glo Luminescent Cell Viability Assay Kit according to the manufacturer's instructions (Promega Corporation). The data were normalized by the number of viable cells. Absorbance and luminescence values were measured by a GloMax-Multi microplate multimode reader (Promega Corporation).

Western blotting. Total cell lysates were extracted with 1X RIPA buffer and protein concentration was determined by BCA protein assay (Thermo Fisher Scientific, Inc.). The extracted proteins (40 μg/well) were separated on 4-12% NuPAGE gels (Thermo Fisher Scientific, Inc.) and then transferred to polyvinylidene fluoride membrane (GE Healthcare Life Sciences). The membranes were blocked with 1X casein solution (cat. no. 37528; Thermo Fisher Scientific, Inc.) for 2 h at room temperature, incubated overnight at 4°C with primary antibodies, and then with horseradish-peroxidase (HRP)-conjugated secondary antibodies for 2 h at room temperature. Reactive proteins were visualized with an enhanced chemiluminescence detection kit (Cyanagen Srl) using X-ray film. TINA 2.09 software (Raytest Isotopenmessgeraete GmbH) was used for densitometric analysis of protein bands in western blots. The following antibodies

were used to detect each protein. Oxphos human WB antibody cocktail (cat. no. 45-8199) and antibodies to HK-I (1:500; cat. no. 2024), HK-II (1:500; cat. no. 2867), PFKP (1:500; cat. no. 8164), pyruvate dehydrogenase (1:500; cat. no. 3205), phosphorylated (p)-MLKL (1:500; cat. no. 91689), p-RIP3 (1:500; cat. no. 93654; 1:500), p-Akt (1:500; cat. no. 9271), Akt (1:500; cat. no. 9272), PARP (1:500; cat. no. 9542), cleaved PARP (1:500; cat. no. 9541), caspase-3 (1:500; cat. no. 14220) and cleaved caspase-3 (1:500; cat. no. 9664) were all purchased from Cell Signaling Technology, Inc. and used for antigen detection. Goat anti-rabbit IgG-HRP (1:5,000; cat. no. sc-2004), goat anti-mouse IgG-HRP (1:5,000; cat. no. sc-2005) and anti-p53 antibody (1:500 cat. no. sc-126) were all purchased from Santa-Cruz Biotechnology, Inc. The membranes were re-probed using anti-β-actin (1:10,000; cat. no. A2228; Sigma-Aldrich; Merck KGaA), anti-RIP3 (1:1,000; cat. no. 13526; Cell Signaling Technology, Inc.), and anti-MLKL (1:1,000; cat. no. 14993; Cell Signaling Technology, Inc.) as the loading controls.

Measurement of ROS and mitochondrial membrane potential. Cells (10^5 cells/well) were seeded on six-well culture plates and incubated overnight in lactic acid-containing RPMI-1640 medium. Cells were treated with or without 20 μM Ly294002 for 2 h, then 30 μM apigenin was added to each well without removing Ly294002 and incubated for 48 h. After trypsinization, cells were harvested by centrifugation at 500 x g for 7 min, and then resuspended in serum-free RPMI-1640 medium containing 2',7'-dichlorodihydrofluorescein diacetate (10 μM) and rhodamine 123 (30 nM; both from Sigma-Aldrich; Merck KGaA) in the dark at 37°C for 30 min to measure the levels of ROS and mitochondrial membrane potential, respectively. The fluorescence intensity of the cells was measured with a MACSQuant analyzer and MACSQuantify software version 2.5 (Miltenyi Biotec GmbH).

Annexin V-PE binding assay. Analysis of apoptotic and necrotic cell distribution was performed according to the instructions provided with the Muse Annexin V & Dead Cell Assay Kit (cat. no. MCH100105; Merck KGaA). Briefly, cells were treated with or without 20 μM Ly294002 for 2 h, then 30 μM apigenin was added to each well without removing Ly294002 and incubated for 48 h. Cells were trypsinized, and collected in a culture medium supplemented with Muse Annexin V & Dead Cell reagent. The cells were then analyzed with Muse cell analyzer (Merck KGaA). Annexin V-phycoerythrin (PE)-positive apoptotic and 7-AAD-positive necrotic cells were detected using Annexin V-PE and 7-amino-actinomycin D (7-AAD) double staining.

Cell cycle analysis. Cell cycle distribution at each phase was determined via propidium iodide (PI) staining as previously described (18). Briefly, trypsinized cells were centrifuged at 500 x g at 4°C for 7 min and then fixed with 70% ethanol overnight at -20°C. After washing the cells with 1X phosphate-buffered saline (PBS), Muse cell cycle reagent (cat. no. MCH100106; Merck KGaA) containing PI and RNAse was added and allowed to react for 30 min. Data from 10,000 cells were analyzed using the MACSQuant analyzer and MACSQuantify software version 2.5 (MiltenyiBiotec GmbH).

Spheroid culture and viability assay. Spheroid culture was performed in an ultra-low attachment 96-well plates as previously described (18). Briefly, plates seeded with 10^4 cells/well were centrifuged at 500 x g for 10 min to allow cells to cluster in the wells and maintained in complete RPMI-1640 medium containing lactic acid (final concentration: 3.8 μM) for 5 days. Spheroids were treated with or without 20 μM Ly294002 for 2 h, then 30 μM apigenin was added to each well without removing Ly294002 and incubated for 48 h. Green fluorescence of fluorescein diacetate (FDA; Sigma-Aldrich, 5 μg/ml) and red fluorescence for PI (Sigma-Aldrich, 10 μg/ml) were used to detect live and dead cells, respectively. Phase-contrast images were acquired with a Leica inverted microscope. Spheroids were visualized using a Leica EL6000 fluorescence microscope (Leica Microsystems GmbH). Spheroid viability was determined according to the instructions provided with the Enhanced Cell Viability Assay Kit (Young In Frontier Co., Ltd.). Briefly, 10 μl of Cellvia solution was added to each well, kept at room temperature for 1 h, and then mixed for 1 min to dissolve the formed formazan crystal. The amount of formazan formed in living cells was measured spectrophotometrically at 450 nm using a GloMax-Multi microplate multimode reader (Promega Corporation).

Statistical analysis. SPSS version 17.0 software (SPSS, Inc.) was used for statistical analysis of experimental data. Statistical analysis was performed by one-way ANOVA and Tukey's post hoc correction. Data are presented as the mean ± standard deviation (S.D.) for three independent experiments. $P<0.05$ was considered to indicate a statistically significant difference.

Results

Pre-adaptation of MM cells to lactic acid exhibits enhanced glycolytic activity. To evaluate the effect of pre-adaptation to an acidic environment, MSTO-211HAcT and H2452AcT cells were cultured for 24, 48 and 72 h in media containing 3.8 μM lactic acid. During this period, the proliferative status was measured and compared with their parental MSTO-211H and H2452 cells. As demonstrated in Fig. 1A, MSTO-211HAcT and H2452AcT cells showed significantly faster growth. Pre-adaptation also increased the tolerance to the anticancer drug gemcitabine at 48 h treatment (Fig. 1B). In addition, the levels of several rate-limiting enzymes in glucose metabolism, including HK-I, HK-II, phosphofructokinase platelet (PFKP) and PDH, were apparently upregulated in both cell types (Fig. 1C). Consistent with the results of western blotting, the activities of HK and PDH were also increased in culture for 48 h (Fig. 1D). Next, the levels of the five complexes in the mitochondrial electron transport chain (ETC) were analyzed. A slight increase was observed in complexes I (NDUFB8, NADH:ubiquinone oxidoreductase subunit B8), III (UQCRC2, ubiquinone-cytochrome C reductase core protein 2), and IV (COX II, mitochondrial cytochrome C oxidase subunit I) in apigenin-treated MSTO-211HAcT and H2452AcT cells when compared with MSTO-211H and H2452 cells (Fig. 1E). Significant upregulation of p-Akt and downregulation of p53, which are potential signaling pathways involved in glycolysis, were observed in MSTO-211HAcT and H2452AcT cells (Fig. 1F).
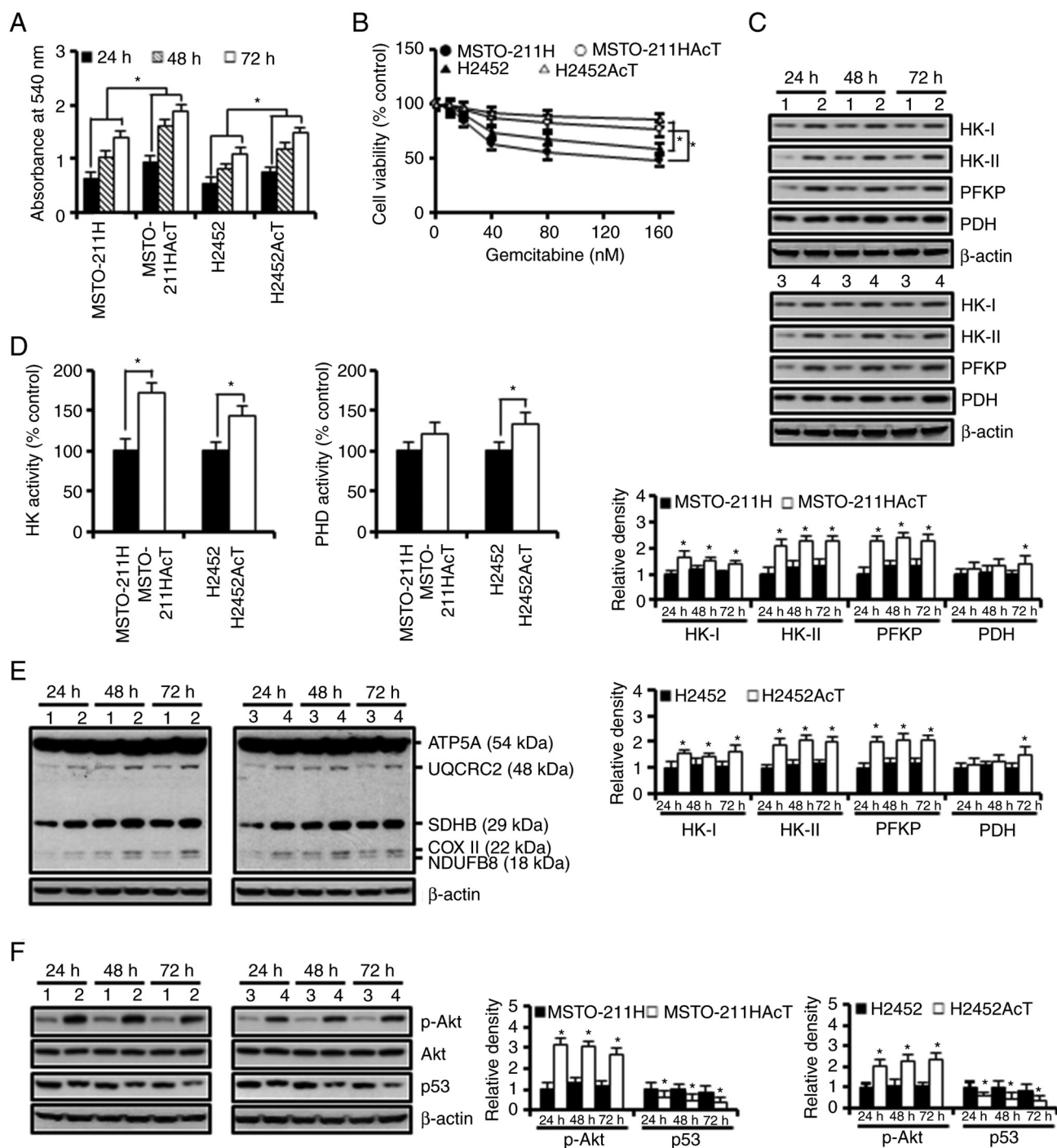
Figure 1. Enhancement of the Warburg-like phenotype in MSTO-211HAcT and H2452AcT cells pre-adapted to lactic acid. Cells were cultured in the complete medium containing 3.8 μM lactic acid for the indicated times, otherwise 48 h. (A) Cell viability was measured by MTT assay during cell culture for 72 h. (B) Cells were treated with increasing concentrations of gemcitabine, followed by MTT assay to measure cell viability. (C) The expression levels of rate-limiting enzymes in glucose metabolism. (D) Activities of hexokinase and pyruvate dehydrogenase. (E) The expression levels of complexes I-V in mitochondrial electron transport chain. (F) The levels of p-Akt, Akt, and p53 proteins. Bar graphs present densitometric analysis of western blot images normalized to β-actin. *P<0.05 vs. respective MSTO-211H or H2452 cells. 1, MSTO-211H; 2, MSTO-211HAcT; 3, H2452; 4, H2452AcT; APG, apigenin; HK, hexokinase; PFKP, phosphofructokinase platelet; PDH, pyruvate dehydrogenase; NDUFB8, NADH-ubiquinone oxidoreductase subunit B8 (complex I); SDHB, succinate dehydrogenase complex iron sulfur subunit B (complex II); UQCRC2, ubiquinone-cytochrome C reductase core protein 2 (complex III); COX II, mitochondrial cytochrome C oxidase subunit II (complex IV); ATP5A, ATP synthase F1 subunit alpha (complex V); p-, phosphorylated.

Apigenin and/or Ly294002 treatment induces apoptosis and necroptosis. To determine the role of Akt as an upstream signaling molecule regulated by apigenin in MSTO-211HAcT and H2452AcT cells, the additive effect of PI3-kinase/Akt inhibition on apigenin-induced cell death was investigated after pre-inhibition of the PI3-kinase using Ly294002 in cultures

containing 3.8 μM lactic acid. An MTT assay was performed to determine the viability of these cells upon treatment with increasing concentrations of apigenin for 48 h. As revealed in Fig. 2A, the half maximal inhibitory concentration values for MSTO-211HAcT and H2452AcT cells were measured to be 47.17 and 56.01 μM, respectively. A concentration of 30 μM, which
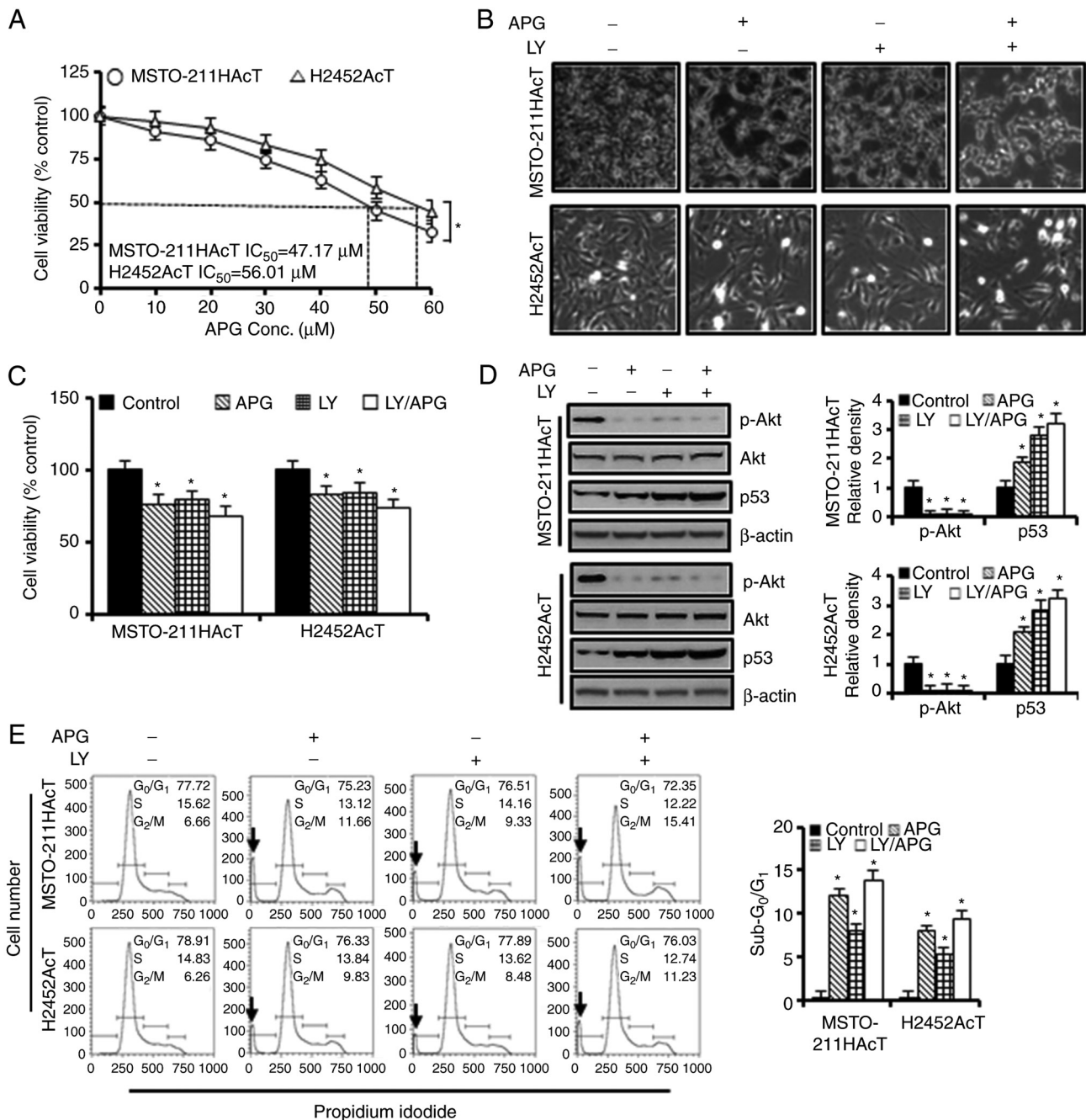
Figure 2. Cytotoxic effects of apigenin and/or Ly294002 on MSTO-211HAcT and H2452AcT cells. (A) Cells were treated with increasing concentrations of apigenin (0, 10, 20, 30, 40, 50 and 60 μM) for 48 h. The percentage of viable cells was determined by comparison with the results obtained using DMSO-treated control cells (100%). Cells were treated with or without Ly294002 (20 μM, 2 h) prior to apigenin treatment (30 μM, 48 h) in RPMI-1640 medium containing 3.8 μM lactic acid. (B) Cell morphology. (C) Percentage of cell viability. (D) The levels of p-Akt and p53 proteins. (E) Cell cycle distribution at each phase. *P<0.05 vs. respective control cells. Arrows indicate sub-G_0/G_1 peak. APG, apigenin; LY, Ly294002; p-, phosphorylated.

showed cell viability in the range of 75-85%, was selected and used for further experiments. The concentration for Ly294002 treatment was determined to be 20 μM, which is a concentration that significantly downregulated p-Akt by western blotting (Fig. S1).

The majority of control cells adhered to cell culture plates, but when cells were exposed to Ly294002 and/or apigenin for 48 h, the cells detached from the surface of the culture plate, increasing the number of cells floating in the culture medium (Fig. 2B). Treatment with apigenin (30 μM) and Ly294002 (20 μM) alone reduced cell viability to 76.19 and 79.59% in MSTO-211HAcT

cells and 82.81 and 83.80% in H2452AcT cells, respectively, compared with control cells (Fig. 2C). However, the percentage of cell viability in the combination treatment of apigenin and Ly294002 did not show a synergistic effect compared with the treatment with apigenin or Ly294002 alone. Ly294002 and apigenin, alone or in combination, inhibited Akt phosphorylation and upregulated p53 levels (Fig. 2D). In cell cycle analysis, treatment with apigenin and Ly294002 alone increased the proportion of sub-G_0/G_1 phase, indicative of apoptosis, to 12.18 and 8.04% in MSTO-211HAcT cells, respectively, and to 7.96 and 5.25% in H2452AcT cells, respectively, as well as the percentage of cell
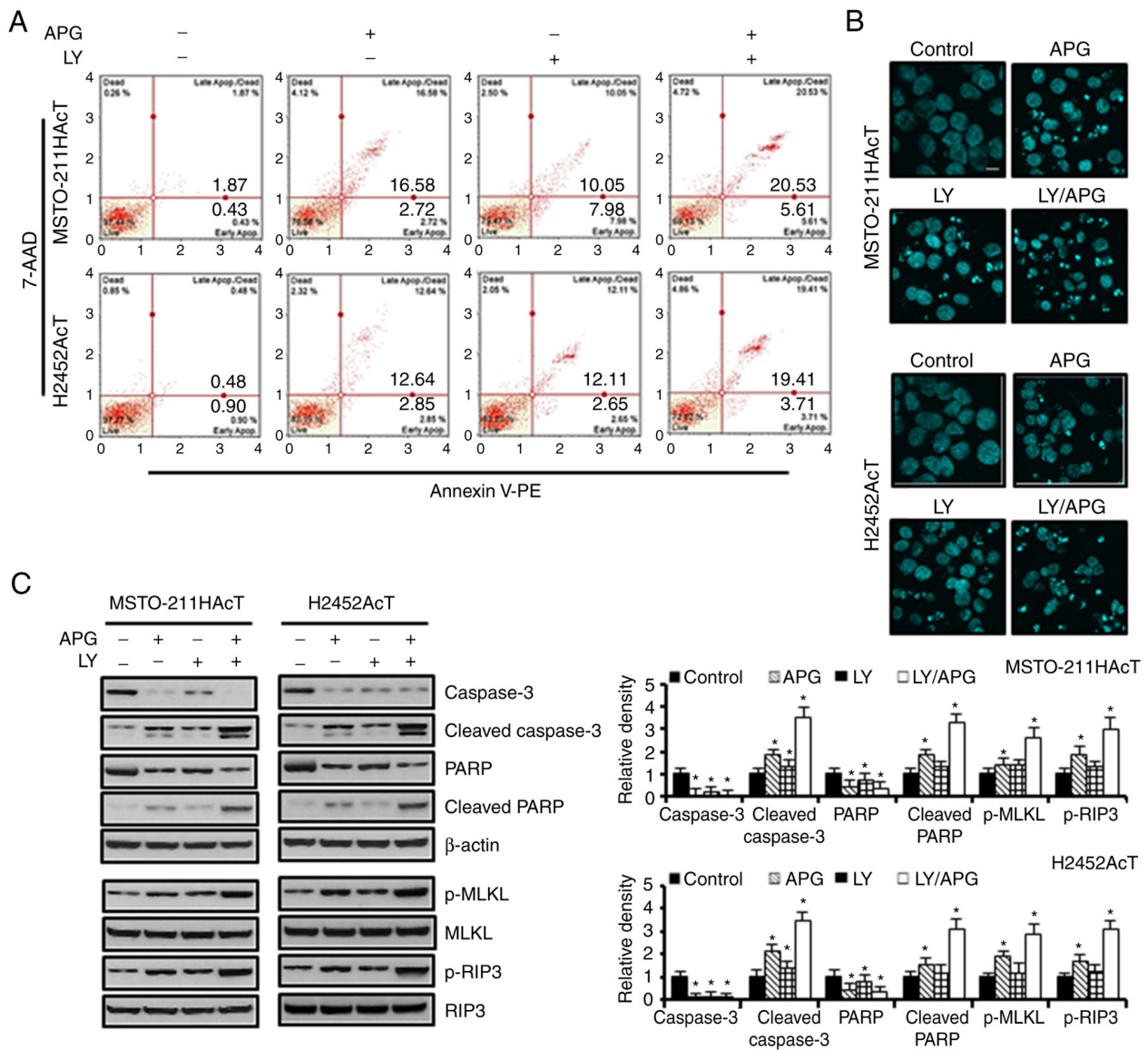
Figure 3. Concurrent induction of apoptosis and necroptosis by apigenin and/or Ly294002 in MSTO-211HAcT and H2452AcT cells. Cells were treated with or without Ly294002 (20 μM, 2 h) prior to apigenin treatment (30 μM, 48 h) in RPMI-1640 medium containing 3.8 μM lactic acid. (A) Fraction of live and dead cells by Annexin V-PE binding assay. (B) Nuclear morphology by DAPI staining (scale bar, 5 μm). (C) The expression levels of apoptosis- and necroptosis-inducing proteins. *P<0.05 vs. respective control cells. Bar graphs present densitometric analysis of western blot images normalized to β-actin. APG, apigenin; LY, Ly294002; p-, phosphorylated.

fraction in the G_2/M phase compared with the controls (Fig. 2E). In Annexin V-PE binding assay of cells treated with apigenin and Ly294002 alone, the percentage of apoptotic cells, including early and late apoptosis, increased to 19.30 and 18.03% in MSTO-211HAcT cells and 15.49 and 14.76%, in H2452AcT cells, respectively, compared with the controls (Fig. 3A). Similarly, nuclear staining with DAPI revealed an increase in the number of cells with the chromatin condensation and nuclear fragmentation (Fig. 3B). Western blot analysis revealed that the levels of proteins responsible for apoptosis, including cleaved caspase-3 and cleaved PARP, and for necroptosis, including p-MLKL and p-RIP3, were upregulated in Ly294002 or apigenin treatment compared with the controls, and that these were enhanced upon combination treatment (Fig. 3C).

Apigenin and/or Ly294002 treatment inhibits ATP production by targeting glycolysis and oxidative phosphorylation. Next,

the effect of apigenin-induced inhibition of the PI3-kinase/Akt pathway on cellular energy metabolism was investigated. Inhibition of the Akt activity by apigenin and/or Ly294002 downregulated the expression of HK-I, HK-II, and PFKP (Fig. 4A) as well as the activities of HK and PDH (Fig. 4B). Next, it was investigated how a decrease in the activity and concentration of these enzymes affected glucose utilization. Treatment with apigenin and Ly294002 alone increased the glucose concentration in the culture medium by 46.91 and 20.58%, respectively, in MSTO-211HAcT cells, and by 32.43 and 14.91%, respectively, in H2452AcT cells (Fig. 4C). Next, it was investigated whether Akt inhibition affected mitochondrial function. After 48-h treatment with apigenin and/or Ly294002, the fraction of cells with the loss of mitochondrial membrane potential, indicative of mitochondrial dysfunction, was increased (Fig. 5A), along with an increase in intracellular ROS levels (Fig. 5B). During this process, the levels of
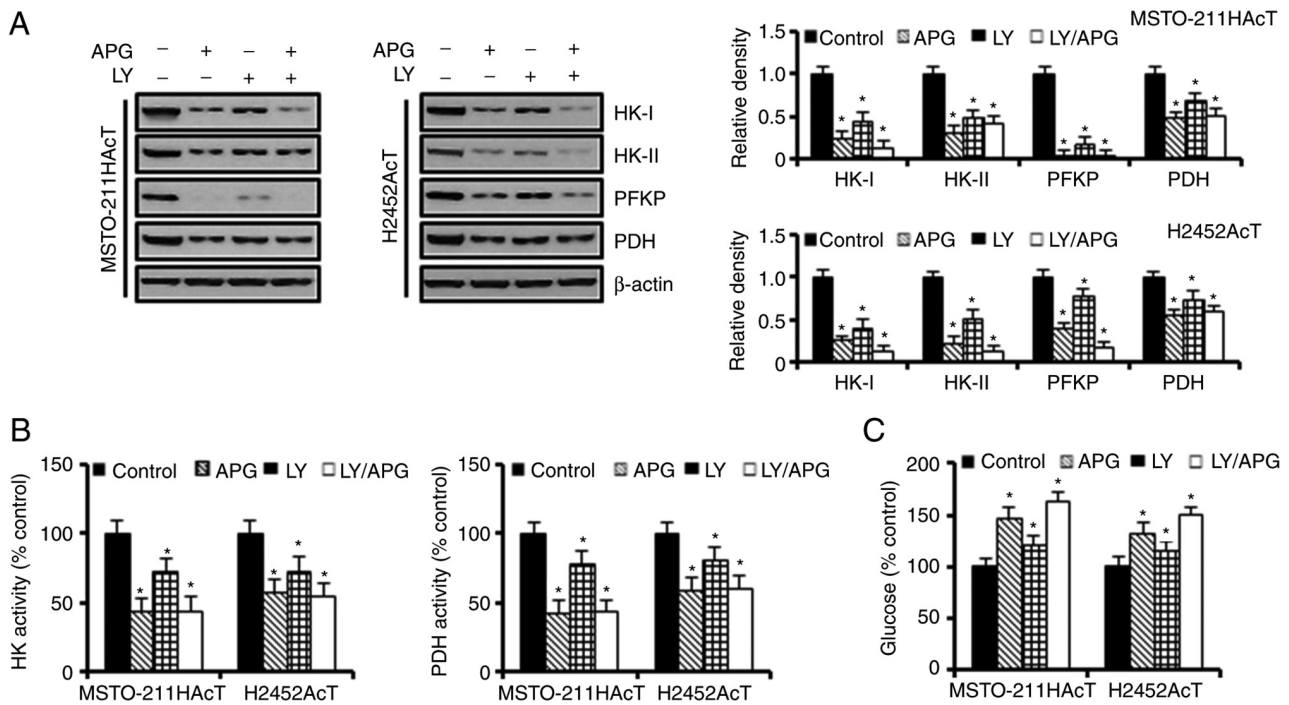
Figure 4. Anti-glycolytic effects of apigenin and/or Ly294002 in MSTO-211HAcT and H2452AcT cells. Cells were treated with or without Ly294002 (20 μM, 2 h) prior to apigenin treatment (30 μM, 48 h) in RPMI-1640 medium containing 3.8 μM lactic acid. (A) The levels of rate-limiting enzymes in glucose metabolism. Bar graphs present densitometric analysis of western blot images normalized to β-actin. (B) Activities of HK and PDH. (C) Glucose concentration in the culture medium. *$P<0.05$ vs. respective control cells. APG, apigenin; LY, Ly294002; PFKP, phosphofructokinase platelet; HK, hexokinase; PDH, pyruvate dehydrogenase.

complexes I-V in ETC (Fig. 5C) and intracellular ATP content (Fig. 5D) were significantly reduced with either apigenin or Ly294002 alone, and the levels were further decreased with the combination treatment.

Apigenin induces anti-glycolytic and cytotoxic effects in 3D spheroid culture. Based on the results of the 2D monolayer cultures, the effect of Akt inhibition on the growth of spheroids and the expression levels of the glycolytic, apoptotic and necroptotic proteins in 3D spheroid cultures were further investigated. A two-color fluorescence assay was used to identify live and dead cells. Cell-permeable FDA is converted into green fluorescent by esterases within living cells, whereas PI enters the nucleus of dead or dying cells and emits red fluorescence upon binding to DNA. As demonstrated in Fig. 6A, Akt inhibition by apigenin and/or Ly294002 decreased spheroid growth with an increase in red fluorescence for PI inside the spheroids indicating dead cells. In addition, the spheroid shape changed from a compact circle in the control group to a less condensed one with an irregular surface. The results of apigenin and/or Ly294002 treatment in 3D cultures revealed similar trends to those in 2D cultures, as shown in reduced spheroid cell viability (Fig. 6B), p-Akt downregulation and p53 upregulation (Fig. 6C), and upregulation of apoptotic proteins, including cleaved caspase-3 and cleaved PARP, necroptotic proteins, including p-MLKL and p-RIP3 (Fig. 6D), and downregulation of key glycolytic enzymes, including HK-I, HK-II, PFKP and PDH (Fig. 6E) compared with controls. However, cells cultured in 3D showed less sensitivity to apigenin and/or Ly294002 compared with those of 2D cultures. Of note, downregulation of p-Akt and upregulation of p53 in response to

Ly294002 was observed to a lesser extent in 3D than in 2D cultures.

Discussion

To further elucidate the cytotoxic mechanism(s) of apigenin, it was investigated whether apigenin targeted enzymes involved in energy metabolism and what the critical upstream signaling pathway is in this process. In the present study, it was found that pre-adaptation of MM cells to an acidic medium containing lactic acid induced a metabolic shift towards enhanced glycolysis, along with Akt activation and p53 downregulation. Apigenin and/or Ly294002 treatment increased both apoptosis and necroptosis of MSTO-211HAcT and H2452AcT cells by downregulating key enzymes of glucose metabolism and inducing mitochondrial dysfunction, at least through Akt inactivation and p53 upregulation. These findings were further validated in 3D spheroid cultures.

Increased cell growth, increased tolerance to the anticancer drug gemcitabine and upregulation of glycolytic enzymes, observed in MM cells pre-adapted to lactic acid-containing medium, suggested the critical role of lactic acid in the metabolic shift to a Warburg phenotype. Recently, it has been demonstrated that pre-culturing of human fibroblasts in medium containing lactic acid promotes the metabolic shift from oxidative phosphorylation to glycolysis by activating transcription of the glycolytic genes through ROS-mediated stabilization of hypoxia inducible factor-1α (HIF-1α) (25). This implies that an increase in lactate concentration may further enhance the dependence of cells on aerobic glycolysis for sustained growth and survival. Enhanced resistance
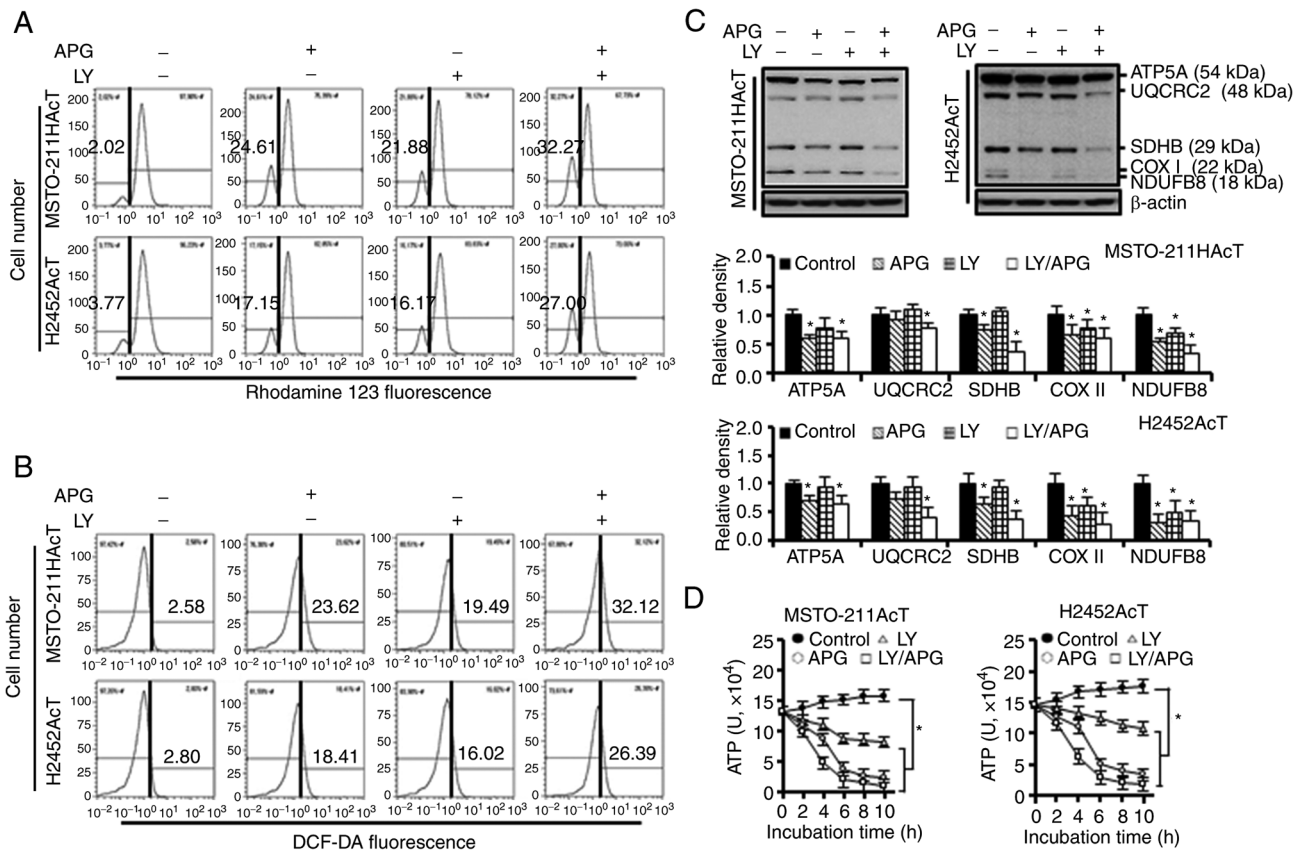
Figure 5. Effects of apigenin and/or Ly294002 on mitochondrial function in MSTO-211HAcT and H2452AcT cells. Cells were treated with or without Ly294002 (20 μM, 2 h) prior to apigenin treatment (30 μM, 48 h) in RPMI-1640 medium containing 3.8 μM lactic acid. (A) Measurement of mitochondrial membrane potential following staining cells with rhodamine123. (B) Measurement of intracellular ROS levels following staining cells with DCF-DA (10 μM). (C) The expression levels of complexes I-V in mitochondrial electron transport chain. Bar graphs present densitometric analysis of western blot images normalized to β-actin. (D) Intracellular ATP levels. *P<0.05 vs. respective control cells. APG, apigenin; LY, Ly294002; NDUFB8, NADH:ubiquinone oxidoreductase subunit B8 (complex I); SDHB, succinate dehydrogenase complex iron sulfur subunit B (complex II); UQCRC2, ubiquinone-cytochrome C reductase core protein 2 (complex III); COX II, mitochondrial cytochrome C oxidase subunit II (complex IV); ATP5A, ATP synthase F1 subunit alpha (complex V), and DCF-DA, 2',7'-dichlorodihydrofluorescein diacetate.

to gemcitabine in MSTO-211HAcT and H2452AcT cells supported previous findings that aerobic glycolysis lead to chemoresistance (26,27). Gemcitabine is an anticancer drug used as standard therapy for MM in combination with cisplatin. Given that chemoresistance is a well-known cause of poor prognosis in the treatment of MM, the development of strategies to reverse resistance to these drugs is essential to improve the therapeutic efficacy of MM.

Aerobic glycolysis, one of the metabolic features found in tumor cells, generates an excess of lactate and H+ in the cytoplasm, which are released extracellularly, causing local acidification (5). Lactic acid was traditionally considered a metabolic waste of anaerobic glycolysis, but has now been described as a key molecule in tumor cell migration, invasion, growth, angiogenesis, chemoresistance and immune escape (28). In this process, a number of signaling pathways and oncogenes, including PI3K/Akt (29), HIF-1 (30) and vascular endothelial growth factor (31) were activated, which contribute to cancer progression. PI3K/Akt signaling is an important regulator of glucose metabolism by enhancing the flux of glycolysis even in normoxic oxidative tumor cells (29). Activation of PI3K/Akt signaling pathway promoted glycolysis and cancer growth by increasing the expression of GLUT-1 and translocation of GLUT-4 to the plasma

membrane, and upregulating the activities of PFK and HK (8). Similarly, PI3K/Akt-mediated upregulation of HK-II expression enhanced anti-apoptotic and pro-proliferative effects by promoting the Warburg effect (8,32). As already mentioned, Akt negatively regulates p53 levels through crosstalk with each other (11,12). Given that p53 mediates cell cycle arrest and associated apoptotic signals, downregulation of p53 may explain part of the potent anti-apoptotic effect of Akt. In addition to its well-known role as a tumor suppressor, p53 mediates negative regulation of HIF-1α, downregulates the expression of GLUT-1, GLUT-4 and HK-II, and upregulates the expression of *TP53*-induced glycolysis and apoptosis regulator, resulting in reduced glycolytic flux (33). Moreover, the p53-deficient cells could produce a significant higher levels of lactate and exhibited a metabolic shift from oxidative phosphorylation to glycolysis (34). Thus, activation of the PI3K/Akt pathway and downregulation of the p53 protein, observed in in MM cells pre-adapted to lactic acid, have been shown to drive metabolic flux towards increased basal glycolysis and enhanced cell growth rate.

Akt inhibition and p53 upregulation in response to apigenin in the current study represent an important mechanism underlying the cytotoxicity of apigenin to MM cells. In line with this finding, blockade of active Akt using Ly294002 demonstrated
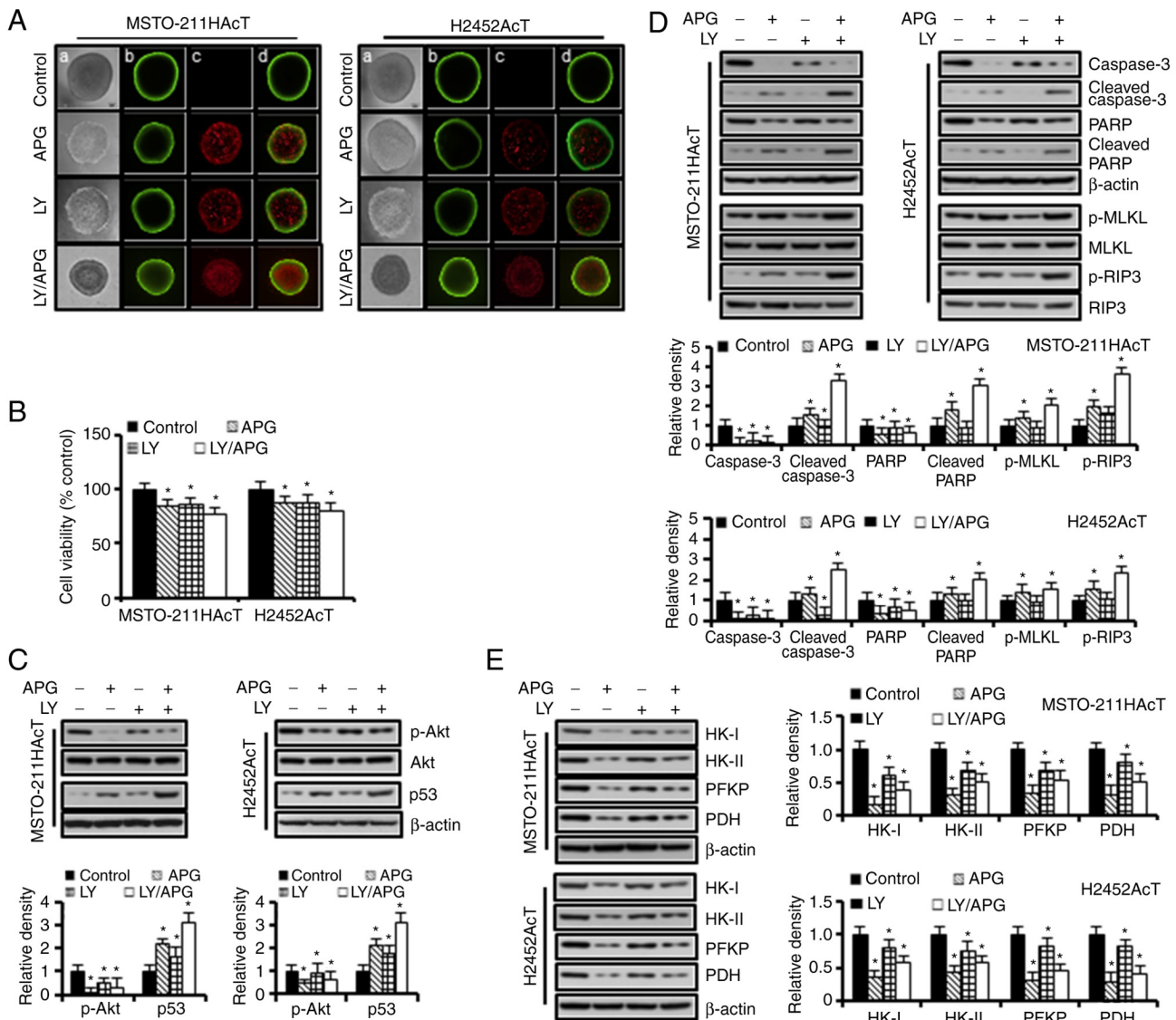
Figure 6. Anti-glycolytic and cytotoxic effects of apigenin and Ly294002 in 3D spheroid culture. Spheroids were cultured in ultralow cluster 96-well plates for 5 days and were then treated with or without Ly294002 (20 μM, 2 h) prior to apigenin treatment (30 μM, 48 h) in RPMI-1640 medium containing 3.8 μM lactic acid for 48 h. (A) Vitality staining of spheroids [from left to right: (a) phase-contrast image, (b) fluorescent images of fluorescein diacetate(+) living cells in green, (c) propidium iodide(+) dead cells in red, and (d) merged]. (B) Spheroid viability. (C) The levels of p-Akt and p53 proteins. (D) The levels of marker proteins for apoptosis and necroptosis. (E) The levels of marker proteins for glycolysis. *P<0.05 vs. respective control cells. Bar graphs present densitometric analysis of western blot images normalized to β-actin. APG, apigenin; LY, Ly294002; HK, hexokinase; PFKP, phosphofructokinase platelet; PDH, pyruvate dehydrogenase; p-, phosphorylated.

the importance of Akt-p53 network in understanding the role of apigenin in both targeting glycolysis and inducing apoptosis and necroptosis of MM cells. Notably, exposure to Ly294002 and apigenin, alone or in combination, increased cytotoxicity, as demonstrated by reduced cell viability together with increased floating cells, increased sub-G_0/G_1 peak with a transient delay in the G_2/M phase, increased Annexin V-PE(+) cell fraction, chromatin condensation and nuclear fragmentation on DAPI staining, and upregulation of apoptosis-and necroptosis-inducing molecules. However, the combination of apigenin and Ly294002 further potentiated the apoptotic, necroptotic, and anti-glycolytic effects compared with apigenin or Ly294002 alone, with certain synergistic effects. It suggested that a series of cellular responses to induce apigenin-induced cytotoxicity are mediated primarily through inhibition of the PI3K/Akt pathway, but other factors or potential pathways,

including the NF-kB, MAPK/ERK and c-JNK pathways, may also be involved in this process (15,17).

Apigenin and/or Ly294002 also downregulated HK-I, HK-II and PFKP, which are rate-limiting enzymes in glycolysis. Increased glucose concentrations in culture medium of apigenin and/or Ly294002-treated group indicates a decrease in glucose utilization, corroborating the results of western blotting showing inhibition of the glycolytic pathway. Downregulation of oxidative phosphorylation enzymes and loss of mitochondrial membrane potential, indicative of mitochondrial dysfunction, limit the ATP production and consequently induce ATP depletion in cells treated with apigenin alone or with Ly294002. Mitochondria play a pivotal role in maintaining cellular redox homeostasis and energy levels and in regulating various types of cell death, including apoptosis and necroptosis (35). The apigenin-induced impairment of
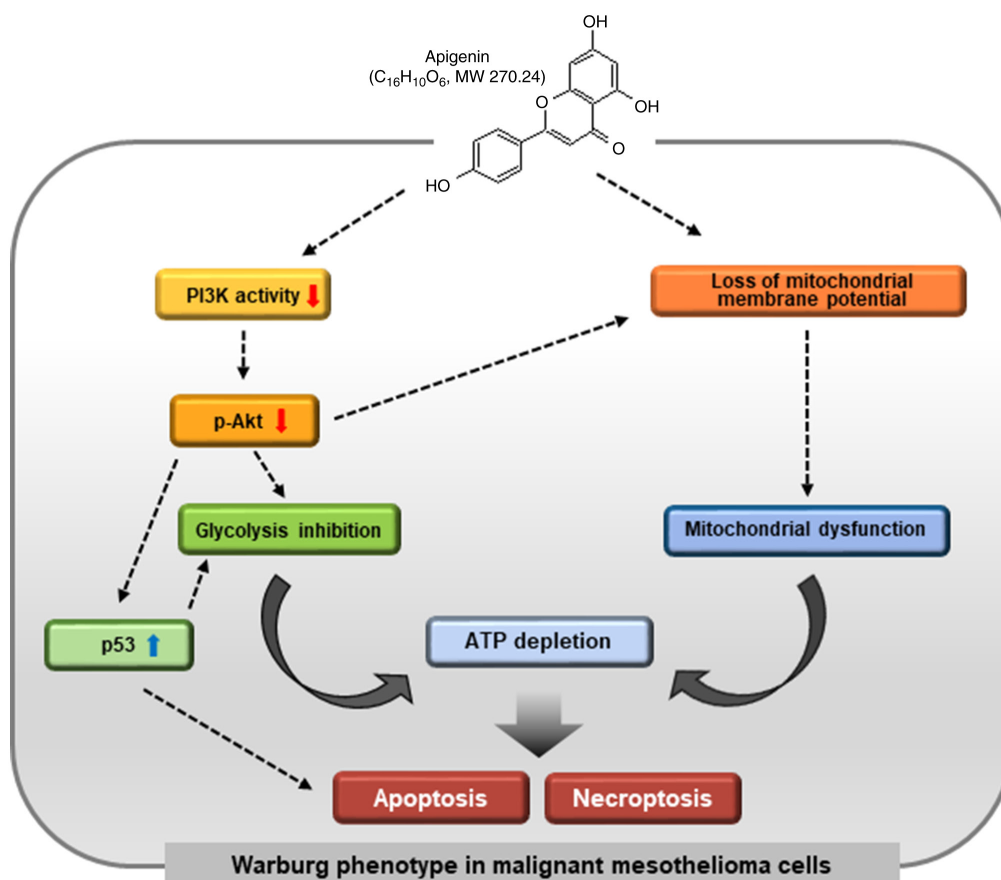
Figure 7. A scheme for apigenin-induced cytotoxicity in malignant mesothelioma cells pre-adapted to lactic acid. Akt inhibition by apigenin causes p53 upregulation, reduced glycolysis, mitochondrial depolarization and cellular ATP depletion, thereby activating executioners leading to apoptosis and necroptosis.

mitochondrial function, observed in the present study, reflects impaired energy metabolism, oxidative damage, and cell death induced by apigenin. Herein, ROS accumulation can foster a vicious cycle that can exacerbate them.

The results of the present study, for the first time to the best of our knowledge, revealed that apigenin-mediated inhibition of Akt leads to reduced glycolysis, and thereby the concurrent induction of apoptosis and necroptosis (Fig. 7). Certain of these results observed in 2D monolayer cultures were also validated in 3D spheroid cultures. However, cells cultured in 3D showed less sensitivity to the effect of apigenin and/or Ly294002 compared with those of 2D cultures. Decreased drug efficacy in 3D cultures has been reported by numerous other researchers, possibly due to reduced drug accessibility to cells due to morphological and/or pathophysiological differences (e.g., local pH) of 3D spheroid structure (36,37). No matter how favorable the results are, *in vitro* study data alone cannot be a reliable indicator of the efficacy of drug candidates, and thus the need for *in vivo* studies through animal experiments is more emphasized. In this regard, the lack of *in vivo* data demonstrates the limitations of the present study, and further studies using animal models are needed to confirm the *in vitro* effects of apigenin.

As aforementioned, cancer cells rely largely on aerobic glycolysis rather than efficient oxidative phosphorylation in glucose metabolism. Given that strategies targeting cancer-specific energy metabolism provide selective growth inhibition in rapidly proliferating cancer cells, as a dual inhibitor targeting both aerobic glycolysis and mitochondrial function, apigenin offers potential clinical advantage as a promising therapeutic candidate for MM. Further studies investigating the metabolic regulation of tumor cells are needed to deepen our understanding of the mechanism(s) involved in apigenin-induced necroptosis.

Acknowledgements

Availability of data and materials

The datasets used and/or analyzed during the current study are available from the corresponding author on reasonable request.

Authors' contributions

SL and SH conceived the present study. YL, MC and SL performed the acquisition, analysis and interpretation of data.

YL and KP conducted all the flow cytometric analysis. SL and YL wrote the original draft. YL and SL confirm the authenticity of all the raw data. All authors provided critical feedback, read and approved the final version of the manuscript. SL were in charge of overall direction and planning.

Ethics approval and consent to participate

Not applicable.

Patient consent for publication

Not applicable.

Competing interests

The authors declare that they have no competing interests.

References

1. Warburg O: The metabolism of carcinoma cells. J Cancer Res 9: 148-163, 1925.
2. Tarrado-Castellarnau M, de Atauri P and Cascante M: Oncogenic regulation of tumor metabolic reprogramming. Oncotarget 7: 62726-62753, 2016.
3. Liberti MV and Locasale JW: The Warburg effect: How does it benefit cancer cells? Trends Biochem Sci 41: 211-218, 2016.
4. Eales KL, Hollinshead KER and Tennantm DA: Hypoxia and metabolic adaptation of cancer cells. Oncogenesis 5: e190, 2016.
5. de la Cruz-López KG, Castro-Muñoz LJ, Reyes-Hernández DO, García-Carrancá A and Manzo-Merino J: Lactate in the regulation of tumor microenvironment and therapeutic approaches. Front Oncol 9: 1143, 2019.
6. Engelman JA, Luo J and Cantley LC: The evolution of phosphatidylinositol 3-kinases as regulators of growth and metabolism. Nat Rev Genet 7: 606-619, 2006.
7. Courtnay R, Ngo DC, Malik N, Ververis K, Tortorella SM and Karagiannis TC: Cancer metabolism and the Warburg effect: The role of HIF-1 and PI3K. Mol Biol Rep 42: 841-851, 2015.
8. Wu Z, Wu J, Zhao Q, Fu S and Jin J: Emerging roles of aerobic glycolysis in breast cancer. Clin Transl Oncol 22: 631-646, 2020.
9. Elstrom RL, Bauer DE, Buzzai M, Karnauskas R, Harris MH, Plas DR, Zhuang H, Cinalli RM, Alavi A, Rudin CM and Thompson CB: Akt stimulates aerobic glycolysis in cancer cells. Cancer Res 64: 3892-3899, 2004.
10. Urso L, Cavallari I, Sharova E, Ciccarese F, Pasello G and Ciminale V: Metabolic rewiring and redox alterations in malignant pleural mesothelioma. Br J Cancer 122: 52-61, 2020.
11. Abraham AG and O'Neill E: PI3K/Akt-mediated regulation of p53 in cancer. Biochem Soc Trans 42: 798-803, 2014.
12. Naderali E, Valipour B, Khaki AA, Rad JS, Alihemmati A, Rahmati M and Charoudeh HN: Positive effects of PI3K/Akt signaling inhibition on PTEN and p53 in prevention of acute lymphoblastic leukemia tumor cells. Adv Pharm Bull 9: 470-480, 2019.
13. Song M, Bode AM, Dong Z and Lee MH: AKT as a therapeutic target for cancer. Cancer Res 79: 1019-1031, 2019.
14. Ahmed SA, Parama D, Daimari E, Girisa S, Banik K, Harsha C, Dutta U and Kunnumakkara AB: Rationalizing the therapeutic potential of apigenin against cancer. Life Sci 267: 118814, 2021.
15. Madunić J, Madunić IV, Gajski G, Popić J and Garaj-Vrhovac V: Apigenin: A dietary flavonoid with diverse anticancer properties. Cancer Lett 413: 11-22, 2018.
16. Tong X and Pelling JC: Targeting the PI3K/Akt/mTOR axis by apigenin for cancer prevention. Anticancer Agents Med Chem 13: 971-978, 2013.
17. Masuelli L, Benvenuto M, Mattera R, Di Stefano E, Zago E, Taffera G, Tresoldi I, Giganti MG, Frajese GV, Berardi G, et al: In vitro and in vivo anti-tumoral effects of the flavonoid apigenin in malignant mesothelioma. Front Pharmacol 8: 373, 2017.
18. Lee YJ, Park KS, Nam HS, Cho MK and Lee SH: Apigenin causes necroptosis by inducing ROS accumulation, mitochondrial dysfunction, and ATP depletion in malignant mesothelioma cells. Korean J Physiol Pharmacol 24: 493-502, 2020.
19. Xu RH, Pelicano H, Zhou Y, Carew JS, Feng L, Bhalla KN, Keating MJ and Huang P: Inhibition of glycolysis in cancer cells: A novel strategy to overcome drug-resistance associated with mitochondrial respiratory defect and hypoxia. Cancer Res 65: 613-621, 2005.
20. Geschwind JF, Ko YH, Torbenson MS, Magee C and Pedersen PL: Novel therapy for liver cancer: Direct intraarterial injection of a potent inhibitor of ATP production. Cancer Res 62: 3909-3913, 2002.
21. Leist M, Single B, Castoldi AF, Kühnle S and Nicotera P: Intracellular adenosine triphosphate (ATP) concentration: A switch in the decision between apoptosis and necrosis. J Exp Med 185: 1481-1486, 1997.
22. Singhal S, Wiewrodt R, Malden LD, Amin KM, Matzie K, Friedberg J, Kucharczuk JC, Litzky LA, Johnson SW, Kaiser LR and Albelda SM: Gene expression profiling of malignant mesothelioma. Clin Cancer Res 9: 3080-3097, 2003.
23. Bonelli M, Terenziani R, Zoppi S, Fumarola C, La Monica S, Cretella D, Alfieri R, Cavazzoni A, Digiacomo G, Galetti M and Petronini PG: Dual inhibition of CDK4/6 and PI3K/AKT/mTOR signaling impairs energy metabolism in MPM cancer cells. Int J Mol Sci 21: 5165, 2020.
24. Lee YJ and Lee SH: Pro-oxidant activity of sulforaphane and cisplatin potentiates apoptosis and simultaneously promotes autophagy in malignant mesothelioma cells. Mol Med Rep 16: 2133-2141, 2017.
25. Kozlov AM, Lone A, Betts DH and Cumming RC: Lactate preconditioning promotes a HIF-1α-mediated metabolic shift from OXPHOS to glycolysis in normal human diploid fibroblasts. Sci Rep 10: 8388, 2020.
26. Ma L and Zong X: Metabolic symbiosis in chemoresistance: Refocusing the role of aerobic glycolysis. Front Oncol 10: 5, 2020.
27. He J, Xie G, Tong J, Peng Y, Huang H, Li J, Wang N and Liang H: Overexpression of microRNA-122 re-sensitizes 5-FU-resistant colon cancer cells to 5-FU through the inhibition of PKM2 in vitro and in vivo. Cell Biochem Biophys 70: 1343-1350, 2014.
28. Pérez-Tomás R and Pérez-Guillén I: Lactate in the tumor microenvironment: An essential molecule in cancer progression and treatment. Cancers (Basel) 12: 3244, 2020.
29. Ruan GX and Kazlauskas A: Lactate engages receptor tyrosine kinases Axl, Tie2, and vascular endothelial growth factor receptor 2 to activate phosphoinositide 3-kinase/Akt and promote angiogenesis. J Biol Chem 288: 21161-21172, 2013.
30. De Saedeleer CJ, Copetti T, Porporato PE, Verrax J, Feron O and Sonveaux P: Lactate activates HIF-1 in oxidative but not in Warburg-phenotype human tumor cells. PLoS One 7: e46571, 2012.
31. Fukumura D, Xu L, Chen Y, Gohongi T, Seed B and Jain RK: Hypoxia and acidosis independently up-regulate vascular endothelial growth factor transcription in brain tumors in vivo. Cancer Res 61: 6020-6024, 2001.
32. Zhuo B, Li Y, Li Z, Qin H, Sun Q, Zhang F, Shen Y, Shi Y and Wang R: PI3K/Akt signaling mediated hexokinase-2 expression inhibits cell apoptosis and promotes tumor growth in pediatric osteosarcoma. Biochem Biophys Res Commun 464: 401-406, 2015.
33. Simabuco FM, Morale MG, Pavan ICB, Morelli AP, Silva FR and Tamura RE: p53 and metabolism: From mechanism to therapeutics. Oncotarget 9: 23780-23823, 2018.
34. Ma W, Sung HJ, Park JY, Matoba S and Hwang PM: A pivotal role for p53: Balancing aerobic respiration and glycolysis. J Bioenerg Biomembr 39: 243-246, 2007.
35. Xue C, Gu X, Li G, Bao Z and Li L: Mitochondrial mechanisms of necroptosis in liver diseases. Int J Mol Sci 22: 66, 2020.
36. Edmondson R, Broglie JJ, Adcock AF and Yang L: Three-dimensional cell culture systems and their applications in drug discovery and cell-based biosensors. Assay Drug Dev Technol 12: 207-218, 2014.
37. Chitcholtan K, Sykes P and Evans J: The resistance of intracellular mediators to doxorubicin and cisplatin are distinct in 3D and 2D endometrial cancer. J Transl Med 10: 38, 2012.